SCIENCE CHINA
Chemistry

•ARTICLES•

July 2021 Vol.64 No.7: 1177–1183
https://doi.org/10.1007/s11426-021-9977-5

Hierarchical self-assembly of crown ether based metal-carbene cages into multiple stimuli-responsive cross-linked supramolecular metallogel

Zi-En Zhang[1†], Yuan-Yuan An[1,2†], Bo Zheng[1], Jin-Ping Chang[1] & Ying-Feng Han[1*]

[1]*College of Chemistry and Materials Science, Northwest University, Xi'an 710127, China;*
[2]*School of Pharmaceutical Sciences, Nanjing Tech University, Nanjing 211816, China*

Received February 23, 2021; accepted March 10, 2021; published online June 11, 2021

The hierarchical self-assembly (HSA) strategy widely utilized in biological systems has been applied in artificial systems to orchestrate small building blocks into complex functional architectures. The non-interfering interactions glue various building blocks together and produce new species with attractive properties. Herein, we functionalized NHC-based assemblies with orthogonal host–guest interaction to fabricate metal-carbene based supramolecular polymer gel. A series of unique crown ether-appended cylinder-like trinuclear Au^{I} hexacarbene assemblies $[Au_3(\mathbf{L})_2](PF_6)_3$ (**L**=**D1**–**D4**, **A1**–**A4**) were synthesized from the corresponding trisimidazolium salts H_3-**L**$(PF_6)_3$ (**L**=**D1**–**D4**, **A1**–**A4**) in which the N-wingtip of the imidazole moieties were substituted with three identical crown ether groups of different sizes (B15C5, B18C6, B21C7, DB24C8). The gold carbene assembly is able to complex six ammonium salts without disrupting the underlying metal-carbene cylinders. In addition, the supramolecular polymer metallogel featuring a multiple-responsiveness can be formed by using $[Au_3(\mathbf{A4})_2](PF_6)_3$ appended with DB24C8 as the core and bisammonium salt as the cross-linker. The case of introducing orthogonal interaction to NHC moiety by N-wingtip substitution demonstrates the feasibility and the power of such strategy to expand the NHC-based supramolecular system and endow them with novel properties.

N-heterocyclic carbene, metallogel, crown ether, orthogonal interaction

Citation: Zhang ZE, An YY, Zheng B, Chang JP, Han YF. Hierarchical self-assembly of crown ether based metal-carbene cages into multiple stimuli-responsive cross-linked supramolecular metallogel. *Sci China Chem*, 2021, 64: 1177–1183, https://doi.org/10.1007/s11426-021-9977-5

1 Introduction

Crown ethers are a classical type of supramolecular macrocyclic hosts and have been utilized to fabricate supramolecular polymer materials featuring responsive and/or self-healing properties [1]. Recently, it has been reported that a pair of orthogonal noncovalent interactions, the metal–ligand interaction and host–guest interaction of crown ether, has exerted its superiority to glue the discrete supramolecular coordination complexes together and produce stimuli-responsive structures with intriguing performances [2]. For example, Stang and other groups [3] have employed coordination-driven self-assembly methodology to construct metallosupramolecular architectures including two-dimensional (squares, rhomboids, triangles, hexagons, *etc*.) and three-dimensional complexes (prism) with well-defined shapes and sizes. Complexes functionalized with crown ether units were subsequently used as the building block to build hierarchical systems through host–guest complexation, leading to supramolecular metallogel with multiple responsiveness [4], supramolecular polymer with tunable fluores-

†These authors contributed equally to this work
*Corresponding author (email: yfhan@nwu.edu.cn)

cence [5], rotaxane-branched dendrimers featuring enhanced photosensitization [6], *etc*.

Supramolecular coordination complexes have shown its capacity to further build complex functional assemblies [7]. However, Werner-type coordination complexes are dominant, where nitrogen and/or oxygen donors of polydentate ligands like pyridine, carboxylic acid, coordinate with the metal centers to build metallosupramolecular architectures [8]. In recent years, a new class of donors featuring metal–C_{NHC} (NHC, N-heterocyclic carbene) bonds started to emerge and the discrete metallosupramolecular assemblies constructed by poly-NHC ligands have been established [9]. We have been focusing on the design of ligands to develop novel metallosupramolecular poly-NHC assemblies [10]. For example, C_3-symmetric tris-NHC ligands were proved to be a class of robust ligand to fabricate three-dimensional organic cages [11]. Furthermore, the pre-organization of the olefin or coumarin groups in such NHC-based assemblies met the criteria of photochemical reaction perfectly, which facilitated the powerful post-assembly modification (PAMs) to generate novel structures not accessible by other routes [12].

Apart from building new discrete poly-NHC assemblies, utilizing such well-shaped assemblies may bring more functionalities. The strategy mentioned above, the combination of metal–ligand interaction and orthogonal noncovalent interactions [13], is a promising way to obtain functionally diverse materials constructed by NHC-based assemblies. A prerequisite for this approach is the metallosupramolecular structure must be retained when another noncovalent interaction exists and does not interfere with the metal–ligand coordination interaction [13]. There is a high possibility that metal–carbon bonds can function independently with another noncovalent interaction. The diverse and controllable host–guest chemistry of crown ethers drives us to combine it with metal-carbene assemblies, which can expand the NHC-based metallosupramolecular system and endow them with novel properties. Herein, we designed a series of trigonal pre-ligands H_3-**L**$(PF_6)_3$ (**L**=**D1**–**D4**, **A1**–**A4**), where N-crown ethers connect next to trisimidazolium salts. These precursors can be transformed into cylinder-like trinuclear Ag^I hexacarbene assemblies $[Ag_3(\mathbf{L})_2](PF_6)_3$ (**L**=**D1**–**D4**, **A1**–**A4**) through the reaction with Ag_2O, and subsequently transmetallate with [AuCl(THT)] (THT=tetrahydrothiophene) to form $[Au_3(\mathbf{L})_2](PF_6)_3$ (**L**= **D1**–**D4**, **A1**–**A4**). Furthermore, we found that only trinuclear Au^I hexacarbene assemblies maintained the cylinder structure when the host-guest interaction was present, and the host-guest complexation was not interrupted by the trinuclear Au^I hexacarbene assemblies. Supramolecular polymeric material was further achieved based on the host-guest interaction between the DB24C8-decorated NHC-metal complex ($[Au_3(\mathbf{A4})_2](PF_6)_3$) and a secondary bisammonium salt.

2 Results and discussion

2.1 Ligand design and synthesis

For this new system, different crown ethers featuring different cavity sizes were systematically studied to build the fundamental poly-NHC library. Firstly, according to the reported procedure a series of benzyl chloride functionalized crown ether moieties including B15C5, B18C6, B21C7 and DB24C8 were prepared [14]. These benzyl chlorides reacted with 2,4,6-tris[4-(1*H*-imidazol-1-yl)phenyl]-1,3,5-triazine or 2,4,6-tris[4-(1*H*-imidazol-1-yl)phenyl]-1,3,5-benzene, following anion exchange with tetrabutylammonium hexafluorophosphate to obtain corresponding trisimidazolium salts H_3-**L**$(PF_6)_3$ (**L**=**D1**–**D4**, **A1**–**A4**) in 85%–89% yields (Supporting Information online). Trisimidazolium salts H_3-**L**$(PF_6)_3$ (**L**=**D1**–**D4**, **A1**–**A4**) were fully characterized by ^1H, $^{13}C\{^1H\}$ nuclear magnetic resonance (NMR) spectroscopy and high resolution-electrospray ionization (HR-ESI) mass spectrometry (Figures S1–S24, Supporting Information online). Typical resonances for the imidazolium N–C*H*–N protons around δ=9.00 ppm were observed in their ^1H NMR spectra (in CD_3CN).

2.2 Construction of N-crown ether-appended trinuclear hexacarbene assemblies

The reaction of the trisimidazolium salts H_3-**L**$(PF_6)_3$ (**L**=**D1**–**D4**, **A1**–**A4**) and Ag_2O in acetonitrile at 70 °C under exclusion of light yielded trinuclear Ag^I hexacarbene assemblies. Then, transmetallation of these trinuclear Ag^I hexacarbene assemblies with [AuCl(THT)] in CH_3CN at ambient temperature resulted in the formation of the corresponding trinuclear Au^I hexacarbene assemblies $[Au_3(\mathbf{L})_2](PF_6)_3$ (**L**=**D1**–**D4**, **A1**–**A4**), in which six crown ethers were appended on the N-wingtip (Scheme 1). The overall yields of complexes $[Au_3(\mathbf{L})_2](PF_6)_3$ (**L**=**D1**–**D4**, **A1**–**A4**) for two steps were 69%–75%. NMR spectroscopy (^1H, $^{13}C\{^1H\}$ and 2D NMR) and HR-ESI mass spectrometry were used to characterize these complexes $[Au_3(\mathbf{L})_2](PF_6)_3$ (**L**=**D1**–**D4**, **A1**–**A4**) (Figures S28–S67). The ^1H NMR spectrum of $[Au_3(\mathbf{L})_2](PF_6)_3$ (**L**=**D1**–**D4**, **A1**–**A4**) showed no resonance signals for imidazolium N–C*H*–N protons which suggested the complete deprotonation of the imidazolium units and the formation of Au–C_{NHC} bonds. For instance, the typical C_{NHC} resonances of $[Au_3(\mathbf{D3})_2](PF_6)_3$ were observed at δ= 183.1 ppm that was consistent with previous reports [12]. Moreover, in the HR-ESI spectrum the corresponding peak assigned to $[Au_3(\mathbf{D3})_2](PF_6)_3$ can be found *m*/*z*=1270.1699 (calcd. for $[Au_3(\mathbf{D3})_2]^{3+}$ 1270.1394) which was in good agreement with its theoretical distribution. Single crystals of trinuclear Au^I hexacarbene assemblies suitable for X-ray analysis cannot be obtained after many attempts. However,

based on our previous work [12], these data unambiguously supported that the structures of these trinuclear Au^I hexacarbene assemblies are cylinder-like complexes, as depicted in Scheme 1.

2.3 Hexakis[2]pseudorotaxanes

Since crown ether-based recognition motifs have been widely employed to fabricate supramolecular assemblies with interesting properties [2], we set to explore their host-guest chemistry in this new system. It is of great importance to ensure that the co-existence of these two interactions does not interfere with each other. The structure of the NHC-assembly should be retained and the host-guest interaction between crown ethers and ammonium salts should be unaffected.

Based on our previous work [11], trinuclear Ag^I hexacarbene assemblies are quite stable and can undergo social self-sorting *via* donor-acceptor π···π stacking interaction between the electron-rich and electron-poor ligands. Hence, at the beginning we planned to introduce host-guest interaction to trinuclear Ag^I hexacarbene assembly $[Ag_3(\mathbf{D3})_2](PF_6)_3$ bearing B21C7, which was reported by Huang and coworkers [15] that dialkylammonium salt could thread into its cavity to form a (pseudo)rotaxane. Complex $[Ag_3(\mathbf{D3})_2](PF_6)_3$ was isolated and purified (Figures S25–S27). After the addition of *N*-benzylbutan-1-ammonium salt **G1** to a solution of $[Ag_3(\mathbf{D3})_2](PF_6)_3$ (CD_3CN:CD_2Cl_2=1:1), though new peaks assigned to the host-guest complex was found in the NMR spectrum, an unexpected peak at 9.02 ppm which was the typical resonances of the imidazolium N–C*H*–N protons also emerged (Figure S77). This indicated that the Ag^I carbene assembly partially collapsed in the presence of ammonium guest. Hence, we synthesized corresponding trinuclear Au^I hexacarbene assemblies $[Au_3(\mathbf{L})_2](PF_6)_3$ (**L**=**D3**, **D4**, **A3**, **A4**) by transmetallation reaction. The complexation experiments were conducted again. Taking $[Au_3(\mathbf{A3})_2](PF_6)_3$ as an example, by employing ^1H-^1H COSY experiment (Figure S78) and the comparison of the spectra of B21C7 and ammonium salt (Figure 1), the signals of the resulting complex were assigned (*vide infra*). Most importantly, the trinuclear Au^I hexacarbene assembly maintained intact, without the free imidazolium N–C*H*–N proton. Based on this result, we prepared a series of crown ether appended Au^I hexacarbene assemblies to enlarge the library.

The size of the crown ether decisively affects the host-guest chemistry. For the smaller crown ethers, the cavity of them can accommodate alkali metals or form three-point binding mode with a primary ammonium ion (RNH_3^+). The host-guest interaction between B15C5, B18C6 functionalized trinuclear Au^I hexacarbene assemblies $[Au_3(\mathbf{L})_2](PF_6)_3$ (**L**=**D1**, **D2**, **A1**, **A2**) and alkali metal ions such as KPF_6, $NaPF_6$ was investigated. Though no collapsed signals were found, no obvious changes were observed in the ^1H NMR, ultraviolet-visible spectra and fluorescence emission spectra, which hindered further investigations. We focused on the larger crown ethers later on, as the signal changes can be observed and followed. For the larger crown ethers, B21C7 and DB24C8, we could prepare a series of hexakis[2]pseudorotaxanes **5**–**16** based on the host-guest recognition between trinuclear Au^I hexacarbene assemblies $[Au_3(\mathbf{L})_2](PF_6)_3$ (**L**=**D3**, **D4**, **A3**, **A4**) and the ammonium salts **G1**–**G6** (Scheme 2). For example, after the addition of 6.0 equivalent ammonium salt **G1** into a mixed solution (CD_3CN:CD_2Cl_2=1:1) of complex $[Au_3(\mathbf{A3})_2](PF_6)_3$ (6.0 mM), the ^1H NMR spectrum exhibited three sets of signals belonging to uncomplexed $[Au_3(\mathbf{A3})_2](PF_6)_3$, uncomplexed **G1** and the hexakis[2]pseudorotaxane **5**, suggesting slow exchange on the NMR time scale. Characteristic shifts caused by the complexation of **G1** and $[Au_3(\mathbf{A3})_2](PF_6)_3$ were observed, where both H_a and H_c protons on **G1** experienced significant downfield shifts (Figure 1). Aromatic protons H_{Ar} shifted upfield due to the shielding effect of the aromatic rings associated with the other units in the complex. For the other

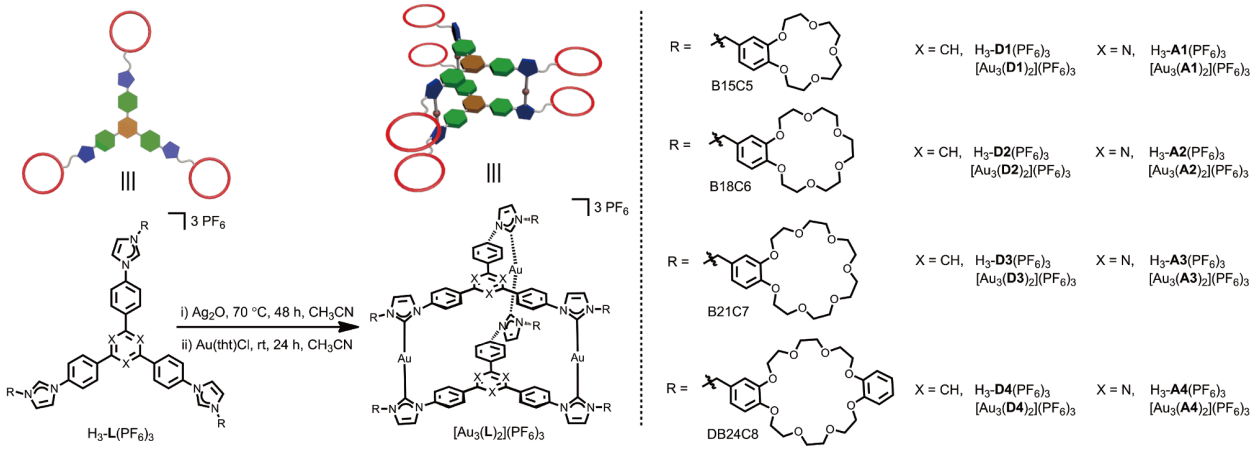

Scheme 1 Synthesis of the eight trinuclear Au^I hexacarbene assemblies $[Au(\mathbf{L})_2](PF_6)_3$ (**L**=**D1**–**D4**, **A1**–**A4**) (color online).

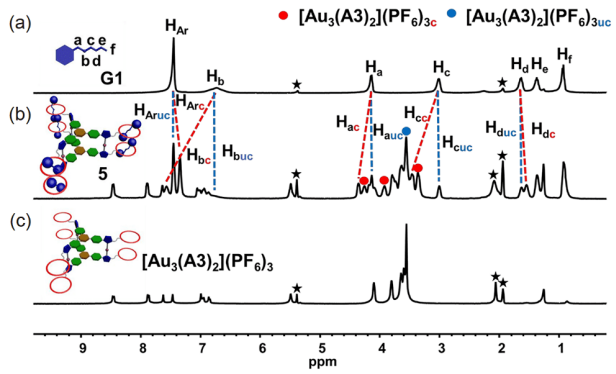

Figure 1 Partial ^{1}H NMR spectra (400 MHz, CD_3CN/CD_2Cl_2 1:1, 298 K) of (a) 36.0 mM secondary dialkylammonium **G1**, (b) 6.0 mM $[Au_3(\mathbf{A3})_2](PF_6)_3$ and 36.0 m**M G1**, and (c) 6.0 mM $[Au_3(\mathbf{A3})_2](PF_6)_3$. Complexed and uncomplexed species are represented by "c" and "uc", respectively. Solvent peaks are marked with an asterisk (color online).

pair of binding moieties, DB24C8 prefers dibenzylammonium salt **G2**. Complex $[Au_3(\mathbf{A4})_2](PF_6)_3$ with DB24C8 was mixed with dibenzylammonium salt **G2**. In the mixture spectrum, it became complicated in CD_3CN:CD_2Cl_2 (*v*/*v*, 1:1) (Figure S82(b)). A downfield shift of the benzylic methylene protons and the splitting and boarding of protons H_α, H_β and H_γ on crown ether were observed. This phenomenon is consistent with the previous reports about the interaction of crown ether and secondary ammonium salts [16]. Additionally, the host-guest interaction between complex $[Au_3(\mathbf{D3})_2](PF_6)_3$ and **G1**, $[Au_3(\mathbf{D4})_2](PF_6)_3$ and **G2** was also studied. The complexation was found to be similar with that between complex $[Au_3(\mathbf{L})_2](PF_6)_3$ (**L**=**A3**, **A4**) and secondary ammonium salts **G1**–**G2** (Figures S80, S84). Furthermore, tetraphenylethylene (TPE)-decorated alkylammonium salts **G3**/**G4** and pyrene-decorated alkylammonium salts **G5**/**G6** were prepared according to the reported procedures [13a]. These fluorescent functional groups were introduced to this new NHC-based metallosupramolecular system to expand the library. The host-guest complexations of $[Au_3(\mathbf{L})_2](PF_6)_3$ (**L**=**D3**, **D4**, **A3**, **A4**) and corresponding guests were all performed and characterized by NMR and fluorescence titration experiments, where similar trend could be observed.

2.4 Supramolecular gel

Supramolecular cross-linked polymer networks prepared by orthogonal coordination-driven self-assembly and noncovalent interactions have received much attention in recent years [2]. Various discrete metallocycles and metallocages coded with different kinds and numbers of secondary recognition moieties interact with their corresponding complementary cross-linkers to form intriguing supramolecular polymer networks [4,5]. The essential metal coordination part is dominated by pyridyl binding motifs. None of the cross-linked supramolecular polymers has been prepared

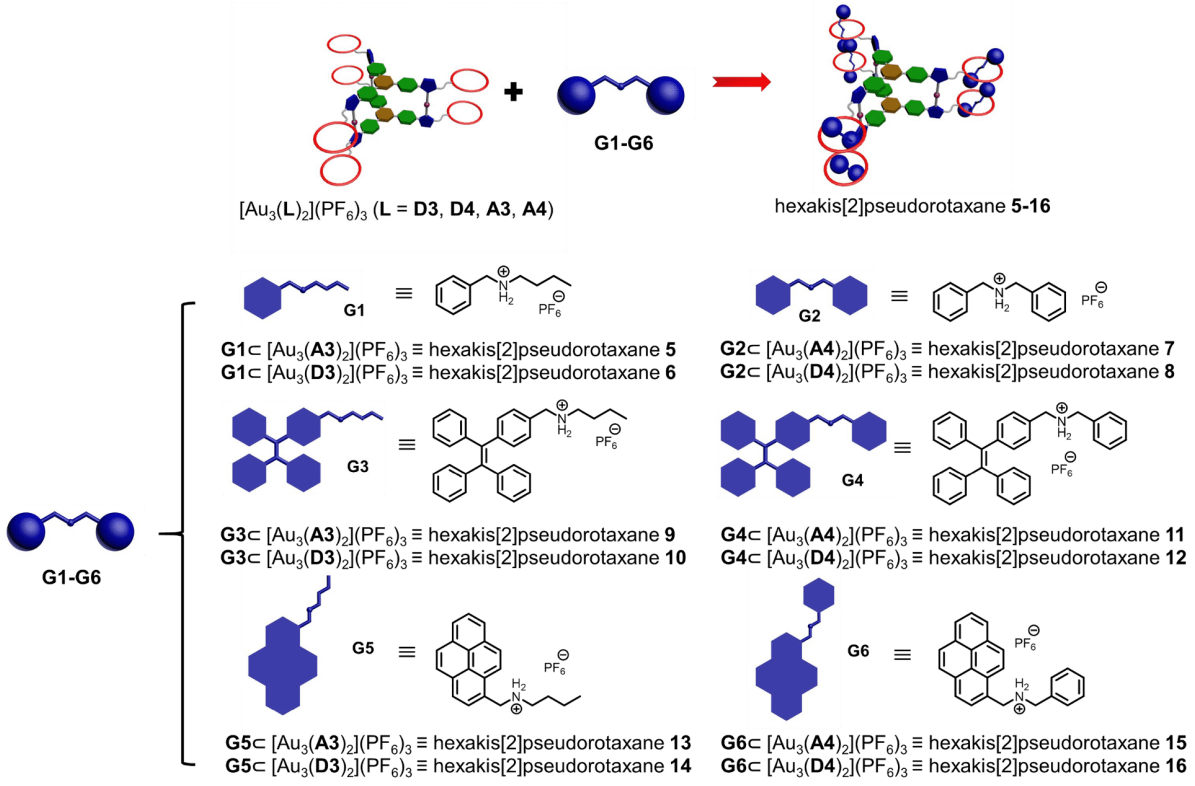

Scheme 2 Formation of hexakis[2]pseudorotaxanes **5**–**16** (color online).

through the hierarchical self-assembly (HSA) involving both metal–carbene coordination and orthogonal crown ether based non-covalent interactions. As the interaction between the secondary ammonium salts and trinuclear Au^I hexacarbene assemblies appended with crown ethers is established, our strategy is to apply this multiple-functionalized core serving as the building block to undergo hierarchical assembly to form a new supramolecular cross-linked polymer networks, as shown in Figure 2 [4,5]. An investigation of the host-guest complexation with the bisammonium salt **G7** with a long alkyl chain spacer in dilute solution with crown ether based trinuclear Au^I hexacarbene assembly $[Au_3(\mathbf{A4})_2](PF_6)_3$ was first carried out. At 20 mM, obvious chemical shift changes were observed by the comparison of the NMR spectra of **G7** and the mixture (Figure S106). We next studied the concentration-dependent ^1H NMR spectra of the two-component system from 2.5 to 100 mM (based on the DB24C8/ammonium salt units). From the obtained ^1H NMR spectra we found that the formation of supramolecular polymer was favored at higher concentration. In addition, the higher the concentration was, the broader the proton signals became, further indicating the formation of high molecular weight polymeric species (Figure 3(a)). Further increasing the concentration of $[Au_3(\mathbf{A4})_2](PF_6)_3$ to 30 mM, metallogel **17** was constructed, where the critical gelation concentration of the supramolecular gel was determined to be 180 mM in crown ether/ammonium salts by repeating the heating and cooling operations until the gel was no longer regenerate. The results of diffusion-ordered NMR spectroscopy (DOSY) further confirmed the formation of cross-linked supramolecular polymer networks (Figure 3(b)). As the concentration of DB24C8/ammonium salt units increased from 10 to 100 mM (based on crown ether units), the measured weight average diffusion coefficient (D) decreased from 2.09×10^{-9} to 8.81×10^{-11} m^2 s^{-1} ($D_{10\ mM}/D_{100\ mM}$=23.72). Generally, supramolecular polymers are considered to be formed when the diffusion coefficient is decreased more than 10-fold [17]. In the supramolecular polymer network, six crown ethers appended in each double-decker structure provide six binding sites and each end of the ditopic bisammonium salt anchors the guest in the cavity of crown ether (Figure 2). However, it is noteworthy that the corresponding trisimidazolium preligand H_3-**A4**$(PF_6)_3$ was not capable to form supramolecular gel with the cross-linker **G7** at the same concentration (based on crown ether units). The participation of rigid metallcages as a linker can even lead to the formation of the gel.

Rheological experiments were also carried out to characterize the obtained gel **17**. Strain scanning test results of the gel showed that as the shear strain increased, the stiffness of the gel increased (Figure 3(d)). When more than 4% of the strain was applied, the storage modulus G' and the loss modulus G'' values dropped rapidly. This can be ascribed to the breakdown of the network. The frequency sweep rheological experiment (Figure 3(e)) showed that G' was larger than G'' at high frequency, where the dynamic cross-links cannot dissociate within such a short time, exhibiting elastic-like behavior; at low frequency, it shows that G'' was larger than G', which suggested the viscous property of the gel [18]. By means of SEM (scanning electron microscopy), the morphology of the supramolecular polymers was also studied. The results of SEM showed a three-dimensional porous network, which further indicated the formation of supramolecular polymer networks (Figure 3(c)).

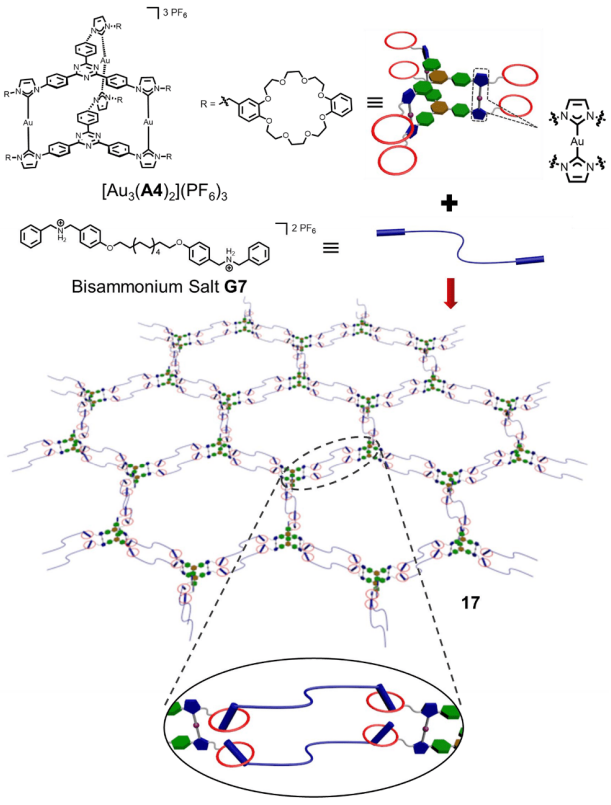

Figure 2 Formation of cross-linked supramolecular polymer network **17** from trinuclear Au^I hexacarbene assembly $[Au_3(\mathbf{A4})_2](PF_6)_3$ and bisammonium salt **G7** (color online).

Due to the reversibility of the host-guest interaction between crown ethers and organic ammonium salts, stimuli-responsiveness of **17** was further explored. Adding and removing K^+, heating and cooling, or adjusting the pH can trigger the reversible sol-gel transition (Figure 4). The qualitative characterization of the thermal reversibility of the gel was confirmed by the inverted vial experiment. The gel collapsed at a high temperature of 55 °C as the decrease of host-guest binding strength and recovered after returning to room temperature due to the recovery of host-guest interaction at low temperature. Upon adding six equivalent amounts of KPF_6, the host-guest interaction between DB24C8 and ammonium was blocked by potassium, thus causing disassembly of the supramolecular network and the formation of sol. Due to the higher affinity of 18-crown-6

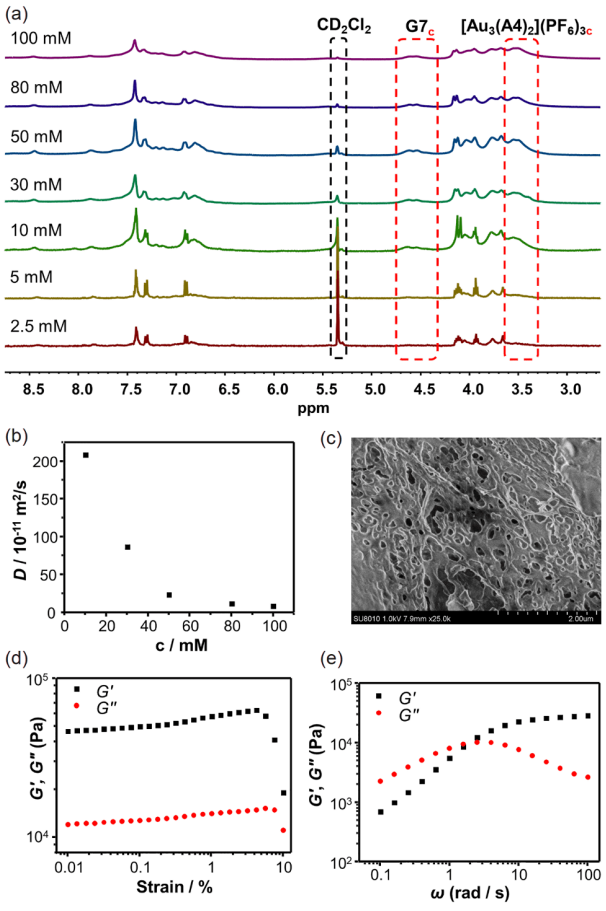

Figure 3 (a) Partial ^{1}H NMR spectra (400 MHz, CD_3CN/CD_2Cl_2 1:1, 298 K) of SPN at different concentrations: 2.5, 5, 10, 30, 50, 80 and 100 mM. (b) Concentration dependence of D (CD_3CN/CD_2Cl_2=1:1, 600 MHz, 298 K) of SPN. (c) SEM image of the SPN prepared by a freeze-drying method. Storage modulus (G') and loss modulus (G'') of the SPN *versus* (d) strain (%) and (e) frequency (ω) for the samples made from 180 mM **17**. Here the concentration refers to that of crown ether units. Complexed species are represented by "c" (color online).

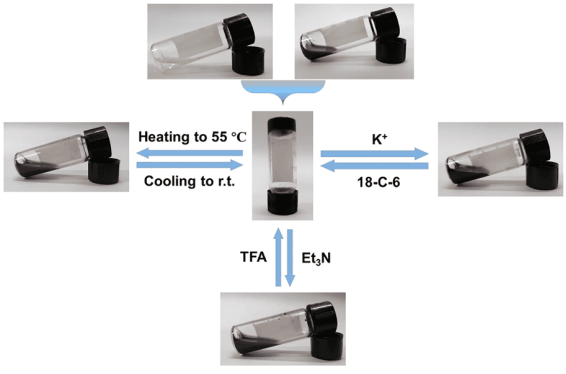

Figure 4 The reversible gel-sol transition of the supramolecular gel (color online).

(18C6) to K^+, an excess of 18C6 was added to extract K^+ from DB24C8, leaving the cavity available for the bisammonium guest, which resulted in the recovery of the gel.

Since the ammonium salt is highly sensitive to acid/base, the host-guest interaction can be controlled by adjusting the pH of the solution, which further leads to the reversible gel-sol transition. As the result, by adding triethylamine (Et_3N), the secondary ammonium salt was deprotonated, causing the disassemble of the gel **17**; the addition of trifluoroacetic acid (TFA) protonated the amine again and restored the metallogel [4,5,17].

3 Conclusions

In summary, we developed a series of Au^I trinuclear hexacarbene assemblies featuring crown ether at each N-wing-tip. By introducing complementary ammonium guests into these gold carbene assemblies, the host-guest complexation formed in an orthogonal fashion which is essential for further applications. Based on that, a big library of trinuclear Au^I hexacarbene assemblies $[Au_3(\mathbf{L})_2](PF_6)_3$ (**L**=**A1**–**A4**, **D1**–**D4**) and metal and organic ammonium guests **G1**–**G6** was established. Furthermore, $[Au_3(\mathbf{A4})_2](PF_6)_3$ appended with DB24C8 served as the core and bisammonium salt **G7** acted as the cross-linker, leading to metal-carbene based supramolecular gel with multiple responsiveness. This provides sufficient proof to demonstrate the feasibility and the power of introducing non-interfering orthogonal interaction to NHC-based assemblies. The NHC donors, non-Werner-type ligands, have been applied to build discrete well-shaped supramolecular complexes, while the combination of the host-guest chemistry of crown ether can further trigger such complexes undergoing hierarchical assembly, obtaining functionally diverse poly-NHC materials. We thus believe this work paves the way for the use of such strategy in the NHC-based supramolecular systems to bring more versatile smart NHC materials.

Acknowledgements This work was supported by the National Natural Science Fund for Distinguished Young Scholars of China (22025107), the National Youth Top-notch Talent Support Program of China, the Key Science and Technology Innovation Team of Shaanxi Province (2019TD-007, 2019JLZ-02), and the FM&EM International Joint Laboratory of Northwest University.

Conflict of interest The authors declare no conflict of interest.

Supporting information The supporting information is available online at http://chem.scichina.com and http://link.springer.com/journal/11426. The supporting materials are published as submitted, without typesetting or editing. The responsibility for scientific accuracy and content remains entirely with the authors.

1 (a) Liu Z, Nalluri SKM, Stoddart JF. *Chem Soc Rev*, 2017, 46: 2459–2478; (b) Xia D, Wang P, Ji X, Khashab NM, Sessler JL, Huang F. *Chem Rev*, 2020, 120: 6070–6123; (c) Ji X, Yao Y, Li J, Yan X, Huang F. *J Am Chem Soc*, 2013, 135: 74–77; (d) Zhou QZ, Jiang HJ,

Ding L, Wang F, Wu T. *Sci China Chem*, 2010, 53: 1081–1088; (e) Chen Y, Huang F, Li ZT, Liu Y. *Sci China Chem*, 2018, 61: 979–992; (f) Yan X, Xu D, Chi X, Chen J, Dong S, Ding X, Yu Y, Huang F. *Adv Mater*, 2012, 24: 362–369; (g) Wang F, Han C, He C, Zhou Q, Zhang J, Wang C, Li N, Huang F. *J Am Chem Soc*, 2008, 130: 11254–11255; (h) Ji X, Dong S, Wei P, Xia D, Huang F. *Adv Mater*, 2013, 25: 5725–5729; (i) Dong S, Luo Y, Yan X, Zheng B, Ding X, Yu Y, Ma Z, Zhao Q, Huang F. *Angew Chem Int Ed*, 2011, 50: 1905–1909

2 (a) Datta S, Saha ML, Stang PJ. *Acc Chem Res*, 2018, 51: 2047–2063; (b) Chen LJ, Yang HB. *Acc Chem Res*, 2018, 51: 2699–2710; (c) Li B, He T, Fan Y, Yuan X, Qiu H, Yin S. *Chem Commun*, 2019, 55: 8036–8059; (d) Cao AM, Hu JS, Wan LJ. *Sci China Chem*, 2012, 55: 2249–2256

3 (a) Sun Y, Chen C, Liu J, Stang PJ. *Chem Soc Rev*, 2020, 49: 3889–3919; (b) Li M, Chen LJ, Cai Y, Luo Q, Li W, Yang HB, Tian H, Zhu WH. *Chem*, 2019, 5: 634–648; (c) Song B, Kandapal S, Gu J, Zhang K, Reese A, Ying Y, Wang L, Wang H, Li Y, Wang M, Lu S, Hao XQ, Li X, Xu B, Li X. *Nat Commun*, 2018, 9: 4575; (d) Chen LJ, Yang HB, Shionoya M. *Chem Soc Rev*, 2017, 46: 2555–2576; (e) Song B, Zhang Z, Wang K, Hsu CH, Bolarinwa O, Wang J, Li Y, Yin GQ, Rivera E, Yang HB, Liu C, Xu B, Li X. *Angew Chem Int Ed*, 2017, 56: 5258–5262

4 Zhang M, Xu D, Yan X, Chen J, Dong S, Zheng B, Huang F. *Angew Chem Int Ed*, 2012, 51: 7011–7015

5 Lu C, Zhang M, Tang D, Yan X, Zhang ZY, Zhou Z, Song B, Wang H, Li X, Yin S, Sepehrpour H, Stang PJ. *J Am Chem Soc*, 2018, 140: 7674–7680

6 Li WJ, Hu Z, Xu L, Wang XQ, Wang W, Yin GQ, Zhang DY, Sun Z, Li X, Sun H, Yang HB. *J Am Chem Soc*, 2020, 142: 16748–16756

7 (a) Ueda Y, Ito H, Fujita D, Fujita M. *J Am Chem Soc*, 2017, 139: 6090–6093; (b) Zarra S, Wood DM, Roberts DA, Nitschke JR. *Chem Soc Rev*, 2015, 44: 419–432; (c) Wu GY, Chen LJ, Xu L, Zhao XL, Yang HB. *Coord Chem Rev*, 2018, 369: 39–75; (d) Li SC, Cai LX, Zhou LP, Guo F, Sun QF. *Sci China Chem*, 2019, 62: 713–718; (e) Sepehrpour H, Fu W, Sun Y, Stang PJ. *J Am Chem Soc*, 2019, 141: 14005–14020; (f) Zhang M, Yin S, Zhang J, Zhou Z, Saha ML, Lu C, Stang PJ. *Proc Natl Acad Sci USA*, 2017, 114: 3044–3049

8 (a) Saha ML, Yan X, Stang PJ. *Acc Chem Res*, 2016, 49: 2527–2539; (b) Mihara N, Ronson TK, Nitschke JR. *Angew Chem Int Ed*, 2019, 58: 12497–12501; (c) Yonesato K, Ito H, Itakura H, Yokogawa D, Kikuchi T, Mizuno N, Yamaguchi K, Suzuki K. *J Am Chem Soc*, 2019, 141: 19550–19554; (d) He L, Wang SC, Lin LT, Cai JY, Li L, Tu TH, Chan YT. *J Am Chem Soc*, 2020, 142: 7134–7144

9 (a) Li Y, An YY, Fan JZ, Liu XX, Li X, Hahn FE, Wang YY, Han YF. *Angew Chem Int Ed*, 2020, 59: 10073–10080; (b) Kuwata S, Hahn FE. *Chem Rev*, 2018, 118: 9642–9677; (c) Cao C, Lang J. *Sci China Chem*, 2019, 62: 655–656; (d) Chen KQ, Sheng H, Liu Q, Shao PL, Chen XY. *Sci China Chem*, 2021, 64: 7–16

10 (a) Gan MM, Liu JQ, Zhang L, Wang YY, Hahn FE, Han YF. *Chem Rev*, 2018, 118: 9587–9641; (b) Zhang YW, Bai S, Wang YY, Han YF. *J Am Chem Soc*, 2020, 142: 13614–13621; (c) Ma LL, An YY, Sun LY, Wang YY, Hahn FE, Han YF. *Angew Chem Int Ed*, 2019, 58: 3986–3991; (d) Sun LY, Feng T, Das R, Hahn FE, Han YF. *Chem Eur J*, 2019, 25: 9764–9770; (e) Li Y, Yang T, Li N, Bai S, Li X, Ma LL, Wang K, Zhang Y, Han YF. *CCS Chem*, 2021, doi: 10.31635/ccschem.021.202100780; (f) Li Y, Yu JG, Ma LL, Li M, An YY, Han YF. *Sci China Chem*, 2021, doi: 10.1007/s11426-020-9937-4

11 (a) Wang YS, Feng T, Wang YY, Hahn FE, Han YF. *Angew Chem Int Ed*, 2018, 57: 15767–15771; (b) AL-Shnani F, Guisado-Barrios G, Sainz D, Peris E. *Organometallics*, 2019, 38: 697–701; (c) Sinha N, Roelfes F, Hepp A, Mejuto C, Peris E, Hahn FE. *Organometallics*, 2014, 33: 6898–6904

12 (a) Sun LY, Sinha N, Yan T, Wang YS, Tan TTY, Yu L, Han YF, Hahn FE. *Angew Chem Int Ed*, 2018, 57: 5161–5165; (b) Gou XX, Liu T, Wang YY, Han YF. *Angew Chem Int Ed*, 2020, 59: 16683–16689; (c) Zhang L, Das R, Li CT, Wang YY, Hahn FE, Hua K, Sun LY, Han YF. *Angew Chem Int Ed*, 2019, 58: 13360–13364

13 (a) Li SL, Xiao T, Lin C, Wang L. *Chem Soc Rev*, 2012, 41: 5950–5968; (b) Elacqua E, Lye DS, Weck M. *Acc Chem Res*, 2014, 47: 2405–2416; (c) Wyman I, Liu GJ. *Sci China Chem*, 2013, 56: 1040–1066; (d) Sun Y, Chen C, Stang PJ. *Acc Chem Res*, 2019, 52: 802–817

14 (a) Wombacher T, Goddard R, Lehmann CW, Schneider JJ. *Dalton Trans*, 2018, 47: 10874–10883; (b) D'Souza F, Chitta R, Gadde S, McCarty AL, Karr PA, Zandler ME, Sandanayaka ASD, Araki Y, Ito O. *J Phys Chem B*, 2006, 110: 5905–5913; (c) Zhang Y, Ouyang Y, Luo Z, Dong S. *Eur J Org Chem*, 2019, 4741–4744; (d) Liu D, Wang D, Wang M, Zheng Y, Koynov K, Auernhammer GK, Butt HJ, Ikeda T. *Macromolecules*, 2013, 46: 4617–4625

15 Zhang C, Li S, Zhang J, Zhu K, Li N, Huang F. *Org Lett*, 2007, 9: 5553–5556

16 (a) Wang W, Zhang Y, Sun B, Chen LJ, Xu XD, Wang M, Li X, Yu Y, Jiang W, Yang HB. *Chem Sci*, 2014, 5: 4554–4560; (b) von Krbek LKS, Roberts DA, Pilgrim BS, Schalley CA, Nitschke JR. *Angew Chem Int Ed*, 2018, 57: 14121–14124; (c) Yang HB, Ghosh K, Northrop BH, Zheng YR, Lyndon MM, Muddiman DC, Stang PJ. *J Am Chem Soc*, 2007, 129: 14187–14189

17 Wang XQ, Wang W, Yin GQ, Wang YX, Zhang CW, Shi JM, Yu Y, Yang HB. *Chem Commun*, 2015, 51: 16813–16816

18 (a) Wang L, Cheng L, Li G, Liu K, Zhang Z, Li P, Dong S, Yu W, Huang F, Yan X. *J Am Chem Soc*, 2020, 142: 2051–2058; (b) Li L, He L, Wang B, Ge P, Jing L, Liu H, Gong C, Zhang B, Zhang J, Bu W. *Chem Commun*, 2018, 54: 8092–8095